A Section 508–conformant HTML version of this article is available at https://doi.org/10.1289/EHP7133.

Long-Term Ambient Air Pollution Exposures and Brain Imaging Markers in Korean Adults: The Environmental Pollution-Induced Neurological EFfects (EPINEF) Study

Jaelim Cho,[1,2,3] Young Noh,[4*] Sun Young Kim,[5] Jungwoo Sohn,[6] Juhwan Noh,[7] Woojin Kim,[7] Seong-Kyung Cho,[7] Hwasun Seo,[7] Gayoung Seo,[7] Seung-Koo Lee,[8] Seongho Seo,[9,10] Sang-Baek Koh,[11] Sung Soo Oh,[11] Hee Jin Kim,[12] Sang Won Seo,[12] Dae-Seock Shin,[13] Nakyoung Kim,[13] Ho Hyun Kim,[14] Jung Il Lee,[15] and Changsoo Kim[2,3,7]*

[1]School of Medicine, University of Auckland, Auckland, New Zealand
[2]Institute of Human Complexity and Systems Science, Yonsei University, Incheon, Republic of Korea
[3]Institute for Environmental Research, Yonsei University College of Medicine, Seoul, Republic of Korea
[4]Department of Neurology, Gachon University Gil Medical Center, Incheon, Republic of Korea
[5]Department of Cancer Control and Population Health, Graduate School of Cancer Science and Policy, National Cancer Center, Goyang, Republic of Korea
[6]Department of Preventive Medicine, Jeonbuk National University Medical School, Jeonju, Republic of Korea
[7]Department of Preventive Medicine, Yonsei University College of Medicine, Seoul, Republic of Korea
[8]Department of Radiology, Severance Hospital, Yonsei University College of Medicine, Seoul, Republic of Korea
[9]Department of Neuroscience, Gachon University College of Medicine, Incheon, Republic of Korea
[10]Department of Electronic Engineering, Pai Chai University, Daejeon, Republic of Korea
[11]Department of Occupational and Environmental Medicine, Wonju Severance Christian Hospital, Wonju College of Medicine, Yonsei University, Wonju, Republic of Korea
[12]Department of Neurology, Samsung Medical Center, Sungkyunkwan University School of Medicine, Seoul, Republic of Korea
[13]MIDAS Information Technology Co., Ltd., Seongnam, Republic of Korea
[14]Department of Integrated Environmental Systems, Pyeongtaek University, Pyeongtaek, Republic of Korea
[15]Korea Testing & Research Institute, Gwacheon, Republic of Korea

Background: Only a limited number of neuroimaging studies have explored the effects of ambient air pollution in adults. The prior studies have investigated only cortical volume, and they have reported mixed findings, particularly for gray matter. Furthermore, the association between nitrogen dioxide (NO_2) and neuroimaging markers has been little studied in adults.

Objectives: We investigated the association between long-term exposure to air pollutants (NO_2, particulate matter (PM) with aerodynamic diameters of $\leq$10 μm (PM10) and $\leq$2.5 μm (PM2.5), and neuroimaging markers.

Methods: The study included 427 men and 530 women dwelling in four cities in the Republic of Korea. Long-term concentrations of PM10, NO_2, and PM2.5 at residential addresses were estimated. Neuroimaging markers (cortical thickness and subcortical volume) were obtained from brain magnetic resonance images. A generalized linear model was used, adjusting for potential confounders.

Results: A 10-$\mu g/m^3$ increase in PM10 was associated with reduced thicknesses in the frontal [–0.02 mm (95% CI: –0.03, –0.01)] and temporal lobes [–0.06 mm (95% CI: –0.07, –0.04)]. A 10-$\mu g/m^3$ increase in PM2.5 was associated with a thinner temporal cortex [–0.18 mm (95% CI: –0.27, –0.08)]. A 10-ppb increase in NO_2 was associated with reduced thicknesses in the global [–0.01 mm (95% CI: –0.01, 0.00)], frontal [–0.02 mm (95% CI: –0.03, –0.01)], parietal [–0.02 mm (95% CI: –0.03, –0.01)], temporal [–0.04 mm (95% CI: –0.05, –0.03)], and insular lobes [–0.01 mm (95% CI: –0.02, 0.00)]. The air pollutants were also associated with increased thicknesses in the occipital and cingulate lobes. Subcortical structures associated with the air pollutants included the thalamus, caudate, pallidum, hippocampus, amygdala, and nucleus accumbens.

Discussion: The findings suggest that long-term exposure to high ambient air pollution may lead to cortical thinning and reduced subcortical volume in adults. https://doi.org/10.1289/EHP7133

Introduction

Recent research has suggested that air pollution is a risk factor for dementia, mild cognitive disorders, and cognitive decline (Chen et al. 2017; Power et al. 2011, 2016; Tzivian et al. 2016; Xu et al. 2016). Only a few studies have linked air pollution to anatomical findings (e.g., cortical volume) on brain magnetic resonance imaging (MRI) in adults, and these studies have yielded contradictory findings regarding gray matter changes related to air pollution (Casanova et al. 2016; Chen et al. 2015; Power et al. 2018). A reason for the discrepancies may be differing brain MRI analysis methods: region of interest (ROI) (Chen et al. 2015) and voxel-based image analyses (Casanova et al. 2016). Another reason may be heterogeneity in the associations between air pollution and brain volumes across geographic regions, as demonstrated in the Atherosclerosis Risk in Communities (ARIC) study analysis (Power et al. 2018). In addition to this inconsistency, the existing evidence is limited to the effect of particulate matter (PM) and there is a paucity of data on the effect of exposure to traffic-related air pollutants, such as nitrogen dioxide (NO_2) on brain imaging markers in adults. An analysis in the Northern Manhattan Study found a null association between NO_2 and brain MRI markers, but the imaging markers were focused on vascular findings, such as white matter hyperintensities (Kulick et al. 2017).

The brain MRI markers used in prior studies were limited to volumetric measures, such as cortical volume—a composite of the genetically different cortical thickness and surface area (Panizzon et al. 2009). Cortical thickness is reportedly a more sensitive indicator of brain structural changes than cortical volume (Burggren et al. 2008; Thambisetty et al. 2010). Some studies investigated

*These authors contributed equally to this work.

Address correspondence to Changsoo Kim, Department of Preventive Medicine, Yonsei University College of Medicine, 50-1 Yonsei-ro, Seodaemun-gu, Seoul, Republic of Korea. Telephone: 82-2-2228-1990. Email: preman@yuhs.ac

Supplemental Material is available online (https://doi.org/10.1289/EHP7133).

The authors declare they have no actual or potential conflicting financial interests.

Received 25 March 2020; Revised 22 October 2020; Accepted 30 October 2020; Published 20 November 2020.

Note to readers with disabilities: *EHP* strives to ensure that all journal content is accessible to all readers. However, some figures and Supplemental Material published in *EHP* articles may not conform to 508 standards due to the complexity of the information being presented. If you need assistance accessing journal content, please contact ehponline@niehs.nih.gov. Our staff will work with you to assess and meet your accessibility needs within 3 working days.

associations between air pollution [elemental carbon, NO_2 (Pujol et al. 2016b), and copper (Pujol et al. 2016a)] and cortical thickness. However, these studies included only children and used 1.5 Tesla brain MRI. Investigating cortical thickness in adults using higher MRI resolution could clarify the mechanism underlying neurodegeneration induced by air pollution exposure.

We examined the association between ambient air pollution (PM and NO_2) and brain MRI markers, including cortical thickness, in adults. To account for the possible impact of differences in individual characteristics between more- and less-polluted areas, we also examined the above association after propensity score matching (PSM) individuals. In addition to ROI-based analysis (with predefined brain regions), we performed surface-based morphometry (SBM) of brain 3 Tesla MRI to capture small (and not predefined) brain regions associated with air pollution.

Methods

Study Participants

The Environmental Pollution-Induced Neurological EFfects (EPINEF) study included four cities in the Republic of Korea—seven wards in two metropolitan cities (Seodaemun-gu, Mapo-gu, Yangcheon-gu, Eunpyeong-gu, Nowon-gu, Gangnam-gu in Seoul; Namdong-gu in Incheon) and two rural cities (Wonju and Pyeongchang). Individuals ≥50 years of age without known neurological diseases (e.g., dementia, movement disorders, stroke) were recruited through local advertisements (starting in 2014) and enrolled. The survey was conducted in three university-based hospitals: Yonsei University Severance Hospital (Seoul), Gachon University Gil Medical Center (Incheon), and Wonju Severance Christian Hospital (Wonju and Pyeongchang). Using a standardized survey protocol, participants underwent questionnaires, anthropometric and blood pressure measurements, blood tests, and the Mini-Mental State Examination (MMSE). Systolic and diastolic blood pressure (in millimeters of mercury) was measured twice and averaged. Blood samples were collected after fasting for ≥12 h and analyzed in a central laboratory (Seoul Clinical Laboratory Co., Ltd, Seoul, Korea). Of the recruited participants from between 2014 and 2017 ($n=1,711$), 998 participants were invited to undergo brain 3T MRI scans by order of enrollment and 2 participants were excluded because of incomplete brain images. After excluding participants with missing values, 957 participants were included in the study. All individuals provided written informed consent. The study was approved by the Yonsei University Health System Institutional Review Board (approval no. 4-2014-0359).

Exposure Assessment

The national prediction model, which included more than 300 geographic variables, was constructed using average annual concentrations of PM with aerodynamic diameters of ≤10 μm (PM10) and NO_2 at approximately 300 air quality regulatory monitoring sites between 2001 and 2016 (Kim and Song 2017). This universal kriging model consisted of mean and variance components. The mean component included two and three summary predictors estimated by partial least squares of more than 300 geographic variables. The variance component was parameterized by range, partial sill, and nugget, which indicated the distance at which spatial correlation, spatial variability, and nonspatial variability existed, respectively. Using this model, we predicted annual average concentrations of each air pollutant at the residential addresses of each study participant. We estimated 5-y average concentrations of the air pollutants prior to the years of the three recruitment intervals (i.e., 2010–2014, 2011–2015, and 2012–2016 for the first, second, and third years of the survey, respectively). The performance of this air pollution prediction model was good for NO_2 and moderate for PM10 (cross-validated $R^2=0.82$ and 0.45, respectively); this prediction ability was comparable to those of national prediction models based on regulatory monitoring data in the United States and Europe (Hart et al. 2009; Vienneau et al. 2010). Concentrations of PM with aerodynamic diameters of ≤2.5 μm (PM2.5) at participants' residential addresses were estimated using the same method as for PM10. In this prediction, the 1-y average in 2015 was computed given that nationwide regulatory monitoring data are available from 2015.

Acquisition and Analysis of Brain MRI

Three-dimensional T1-magnetization prepared rapid gradient echo images were obtained. The imaging parameters used in this study were as follows: repetition time, 1,900 ms; echo time, 2.93 ms; flip angle, 8°; pixel bandwidth, 170 Hz/pixel; matrix size, 256 × 208; field of view, 256 mm; and number of excitations (NEX): 1, total acquisition. ROI-based and SBM analyses of the brain images were performed using the standard pipeline of FreeSurfer (version 6.0.0; http://surfer.nmr.mgh.harvard.edu/). Both analyses involved subcortical segmentation (Fischl et al. 2002, 2004a), cortical surface reconstruction (Dale et al. 1999; Fischl et al. 1999a), cortical thickness mapping (Fischl and Dale 2000), surface-based inter-subject alignment (Fischl et al. 1999a, 1999b), and cortical parcellation (Desikan et al. 2006; Fischl et al. 2004b). Specifically, in the ROI-based analysis, the outer and inner cortical surface meshes were constructed based on the magnetic resonance volume of each individual. These two isomorphic meshes had identical vertices and connectivity because the outer cortical surface was constructed by deforming the inner surface. To establish inter-individual correspondence, each individual's cortical surface to 40,962 vertices in each hemisphere was resampled in line with a previous study (Cho et al. 2012). We used the manifold harmonic transform (MHT), which mapped the cortical thickness from the surface onto the frequency domain (Qiu et al. 2006; Vallet and Lévy 2008). The MHT filtered out high-frequency components (treated as noise), allowing us to remove noise and reduce the dimensionality of the cortical thickness data (Cho et al. 2012). This procedure yielded estimates of regional cortical thickness (frontal, temporal, parietal, occipital, cingulate, and insula) and subcortical gray matter volume (thalamus, caudate, putamen, pallidum, hippocampus, amygdala, and nucleus accumbens). Estimates of the right and left hemispheres were averaged, and global cortical thickness was calculated by averaging the six cortical thicknesses. In contrast to the ROI-based analysis, SBM did not require *a priori* definition of an ROI and enabled the visualization of small brain regions associated with air pollution in the present study. Compared with the voxel-based morphometry used in the study by Casanova et al. (2016), SBM measures more specific metrics, such as cortical thickness. In the preprocessing for SBM, individual thickness maps were resampled on the FreeSurfer reference surface (the so-called fsaverage) and then smoothed along the reference surface, (Fischl et al. 1999b; Hagler et al. 2006). The reference surface was represented by triangulated meshes of the cortex, and the cortical thickness of each vertex (where the points of adjacent triangles meet) was used for hypothesis testing in SBM.

The MRI scanners used included a Philips 3T Achieva MRI scanner ($n=646$) at Yonsei University Severance Hospital and Wonju Severance Christian Hospital and a Siemens 3T Verio MRI scanner ($n=311$) at Gachon University Gil Medical Center. To address potential differences, 12 participants were invited to participate in a pilot study and underwent brain MRI scans using

both scanners. We created linear regression equations, including an average estimate of cortical thicknesses or subcortical volumes from the Siemens scanner as an independent variable and that from the Philips scanner as a dependent variable; here, age was adjusted for. For intracranial volume (ICV), a simple linear regression equation was created. Adjusted R^2 of the regression equations were 0.91 for cortical thickness, 0.93 for cortical volume, and 0.91 for ICV. The resulting equations were used to transform estimates from the Siemens scanner to equivalents of those from the Phillips scanner. The regression coefficients for age and global cortical thickness in the equation for cortical thickness was also applied to the individuals' thickness maps measured on native cortical surfaces.

Covariates

The following covariates were selected *a priori*: age, sex, socioeconomic factors, and cardiovascular risk factors. The socioeconomic factors included education level (years), marital status [living with a spouse or partner (cohabiting) or not], and income level. The cardiovascular risk factors included history of cardiovascular diseases (hypertension, diabetes, hyperlipidemia, and angina or myocardial infarction), smoking (never, former, or current smoker), alcohol consumption (currently drinking or not), walking days per week, body mass index (in kilometers per meter squared), systolic and diastolic blood pressure (in millimeters mercury), fasting blood glucose, and total cholesterol levels.

Statistical Analysis

In the main analysis, a generalized linear model was used to investigate ROI-based brain MRI markers associated with air pollutant concentrations. We estimated linear changes in brain MRI markers per a 10-$\mu g/m^3$ increase in PM and a 10-ppb increase in NO_2 using two models. Model 1 was adjusted for the aforementioned covariates (except for the cardiovascular risk factors) plus survey year and ICV. Model 2 was constructed including the Model 1 variables plus the cardiovascular risk factors (with a view to reporting estimates with and without adjustment for potential intermediates). In this analysis, beta coefficients represented estimated differences in cortical thickness (in millimeters) and subcortical volumes (in millimeters cubed). Considering possible sex differences in cortical thickness and volume (Ritchie et al. 2018), we additionally investigated sex-specific associations between air pollutant concentrations and ROI-based brain MRI markers. The significance of sex difference was tested using the method described by Altman and Bland (2003), yielding $p_{interaction}$ values.

As a post hoc analysis, we conducted PSM to effectively control for the possible impact of differences in individual characteristics between more- and less-polluted areas. In this multicity study, individual characteristics might have been affected by area of residence. Adjusting for or stratifying on area of residence can lead to a loss of sufficient variations in air pollutant concentrations to detect the studied association, particularly in a relatively small study. Furthermore, simple adjustment for area of residence (at the city level) might not account for individual differences between more- and less-polluted areas within a city. The PSM approach, mimic to a randomized intervention (i.e., higher or lower air pollution exposure in this study), enabled us to obtain two comparable groups dwelling in more- and less-polluted areas. Although this approach weakens generalizability by selecting subgroups, it improves comparability and, in turn, the possibility of causal inference in observational studies (Bind 2019). In the present study, the propensity score was defined as the probability to be assigned to the higher or lower exposure group given a set of individual covariates. To obtain PSM pairs for each air pollutant (PM10, PM2.5, or NO_2), we created three subsets of participants. In each subset, we selected those with air pollution concentration percentiles $\geq$66.6 (the higher exposure group) and those with concentration percentiles $\leq$33.3 (the lower exposure group). We then estimated propensity scores using multivariable logistic regression models (including all Model 2 variables except ICV). The resulting *C*-statistics of the logistic models were 0.71 for PM10, 0.72 for PM2.5, and 0.79 for NO_2. Optimal matching was performed within a maximum radius (i.e., absolute difference of propensity score) of 0.1, in which one individual in the lower group was selected for each individual in the higher group. After estimating propensity scores for each air pollutant concentration in the higher (vs. lower) group, the propensity scores for the two groups matched 1:1. Using the resulting PSM subsets, we explored brain MRI markers associated with the higher (vs. lower) air pollution group. In the ROI-based analysis, we used linear mixed models, with the matched pair identifier as a random effect (to account for the correlation between matched pairs) and adjusting for ICV. In SBM (only for cortical thickness), we conducted paired *t*-tests on every vertex of the reference surface, with both false discovery rate (FDR) correction ($p < 0.05$) (Casanova et al. 2016) and cluster-wise correction (Monte-Carlo simulation, threshold with cluster-wise $p < 0.05$) for multiple comparisons (Hagler et al. 2006).

Another post hoc analysis was conducted to examine the associations between PM and brain MRI markers after controlling for NO_2 and vice versa. We built two-pollutant models, including the Model 2 covariates used in the main analysis.

Two sensitivity analyses were performed. First, constrained to cognitively healthy participants ($n = 883$), we repeated the main analysis (Model 2). Although individuals with dementia, movement disorders, or stroke were not eligible to participate in our study, some participants might have had mild cognitive impairment. This means that the entire study population in the present study might not represent cognitively healthy individuals. In this analysis, participants with possible cognitive impairment (defined as an MMSE score <24) were excluded. Second, constrained to participants who underwent the survey from 2015 ($n = 792$), we examined the associations between PM2.5 and brain MRI markers using the Model 2 covariates used in the main analysis. This analysis enabled us to address the issue of temporal misalignment between PM2.5 data (data available from 2015) and brain MRI data, by excluding the participants with MRI data obtained in 2014.

All statistical analyses were conducted using SAS (version 9.4; SAS Institute Inc.) and FreeSurfer (version 6.0). The two-sided $p < 0.05$ was set as statistical significance.

Results

Characteristics of Study Participants

The mean [standard deviation (SD)] age was 67.3 (6.4) y (Table 1). The mean (SD) concentrations of PM10, PM2.5, and NO_2 were 50.7 (4.8) $\mu g/m^3$, 26.0 (0.7) $\mu g/m^3$, and 29 (9.8) ppb, respectively. The correlations between PM10 and PM2.5 ($r = 0.58$, $p < 0.001$), between PM10 and NO_2 ($r = 0.67$, $p < 0.001$), and between PM2.5 and NO_2 ($r = 0.38$, $p < 0.001$) were statistically significant. The mean (SD) global thickness was 2.4 (0.1) mm. The study participants had significantly higher air pollutant concentrations compared with participants who did not undergo brain MRI scans (Table S1). Although some factors (e.g., education level, income, smoking, alcohol consumption) significantly differed between the two groups, there were no significant differences in mean age and MMSE score. Characteristics of the PSM individuals (the higher and lower air pollution groups) are presented in Table

Table 1. Characteristics of study participants.

Characteristics	Total ($n = 957$)		Men ($n = 427$)		Women ($n = 530$)	
Age [mean (SD)]	67.3	(6.4)	68.3	(6.6)	66.4	(6.1)
Education level (y) [mean (SD)]	9.9	(4.3)	10.8	(4.3)	9.2	(4.2)
Marital status: cohabiting [*n* (%)]	804	(84.0)	403	(94.4)	401	(75.7)
Income per month[a] [*n* (%)]						
<$455	95	(9.9)	36	(8.4)	59	(11.1)
$455–$908	123	(12.9)	53	(12.4)	70	(13.2)
$909–$1,363	134	(14)	52	(12.2)	82	(15.5)
$1,364–$1,817	151	(15.8)	69	(16.2)	82	(15.5)
$1,818–$2,726	164	(17.1)	74	(17.3)	90	(17.0)
$2,727–$3,635	110	(11.5)	62	(14.5)	48	(9.1)
$3,636–$5,454	89	(9.3)	44	(10.3)	45	(8.5)
≥$5,455	46	(4.8)	24	(5.6)	22	(4.1)
Missing	45	(4.7)	13	(3.0)	32	(6.0)
History of disease [*n* (%)]						
Hypertension	313	(32.7)	119	(27.9)	194	(36.6)
Diabetes	170	(17.8)	89	(20.8)	81	(15.3)
Hyperlipidemia	308	(32.2)	101	(23.7)	207	(39.1)
Angina or myocardial infarction	89	(9.3)	42	(9.8)	47	(8.9)
Smoking [*n* (%)]						
Never smoker	633	(66.1)	119	(27.9)	514	(97.0)
Former smoker	261	(27.3)	249	(58.3)	12	(2.3)
Current smoker	63	(6.6)	59	(13.8)	4	(0.7)
Alcohol consumption [*n* (%)]	395	(41.3)	252	(59.0)	143	(27.0)
Walking days per week [mean (SD)]	4.7	(2.3)	4.7	(2.3)	4.7	(2.3)
Body mass index (kg/m^2) [mean (SD)]	24.7	(3)	24.7	(2.8)	24.7	(3.1)
Systolic blood pressure (mmHg) [mean (SD)]	128.5	(14.2)	129.2	(13.3)	128.0	(14.9)
Diastolic blood pressure (mmHg) [mean (SD)]	75.2	(9.1)	75.9	(8.6)	74.7	(9.4)
Total cholesterol (mg/dL) [mean (SD)]	183.2	(37.1)	175.9	(38.4)	189.1	(35.0)
Fasting blood glucose (mg/dL) [mean (SD)]	99.9	(21.5)	102.5	(21.5)	97.8	(21.2)
Survey year [*n* (%)]						
First (August 2014–March 2015)	165	(17.2)	67	(15.7)	98	(18.5)
Second (April 2015–March 2016)	381	(39.8)	195	(45.7)	186	(35.1)
Third (April 2016–March 2017)	411	(43)	165	(38.6)	246	(46.4)
PM10 ($\mu g/m^3$)						
Mean (SD)	50.7	(4.8)	50.7	(4.8)	50.7	(4.8)
Range						
Tertile 1	34.5–49.7		34.5–49.7		37.3–49.7	
Tertile 3	52.8–62.2		52.8–62.1		52.9–62.2	
PM2.5 ($\mu g/m^3$)						
Mean (SD)	26.0	(0.7)	25.9	(0.7)	26.0	(0.7)
Range						
Tertile 1	24.1–25.6		24.1–25.6		24.3–25.6	
Tertile 3	26.2–28.1		26.1–28.1		26.2–28.1	
NO_2 (ppb)						
Mean (SD)	29.0	(9.8)	26.5	(10.8)	31.1	(8.4)
Range						
Tertile 1	5.8–29.9		5.8–21.6		5.8–31.2	
Tertile 3	34.5–44.3		33.5–44.3		34.8–44.0	
Cortical thickness (mm) [mean (SD)]						
Global	2.4	(0.1)	2.4	(0.1)	2.5	(0.1)
Frontal	2.5	(0.1)	2.5	(0.1)	2.5	(0.1)
Parietal	2.2	(0.1)	2.2	(0.1)	2.2	(0.1)
Temporal	2.7	(0.1)	2.7	(0.1)	2.7	(0.1)
Occipital	2.0	(0.1)	2.0	(0.1)	2.0	(0.1)
Cingulate	2.5	(0.1)	2.4	(0.1)	2.5	(0.1)
Insula	2.8	(0.1)	2.8	(0.1)	2.8	(0.1)
Subcortical volume (mm^3) [mean (SD)]						
Thalamus	6,462.3	(715.9)	6,669.1	(757.5)	6,295.8	(633.8)
Caudate	3,149.4	(461.5)	3,280.1	(471.3)	3,044.1	(425.7)
Putamen	4,325.2	(520.2)	4,467.6	(541.8)	4,210.5	(472.4)
Pallidum	1,798.1	(219.8)	1,836.4	(217.7)	1,767.3	(216.8)
Hippocampus	3,813.4	(405.9)	3,880.6	(418.3)	3,759.3	(387.6)
Amygdala	1,510.2	(209.3)	1,576.9	(213.9)	1,456.5	(189.4)
Nucleus accumbens	337.8	(105.9)	354.0	(106.8)	324.8	(103.4)
Intracranial volume (1,000 mm^3) [mean (SD)]	1,527.5	(168.0)	1,630.2	(147.7)	1,444.7	(134.4)

Note: NO_2, nitrogen dioxide; PM, particulate matter; PM2.5, PM ≤2.5 μm in aerodynamic diameter; PM10, PM ≤10 μm in aerodynamic diameter; SD, standard deviation.
[a]Income was based on the average exchange rate at 1,100 Korean won per 1 U.S. dollar.

Table 2. Association between air pollution and brain magnetic resonance imaging markers in adults.

			Model 1			Model 2		
Pollutant	Measurement	Brain region	Beta	(95% CI)	*p*-Value	Beta	(95% CI)	*p*-Value
PM10	Cortical thickness (mm)	Global	0.00	(−0.01, 0.01)	0.60	0.00	(−0.01, 0.01)	0.60
		Frontal	−0.02	(−0.03, −0.01)	0.003	−0.02	(−0.03, −0.01)	0.005
		Parietal	0.00	(−0.02, 0.01)	0.68	−0.01	(−0.02, 0.01)	0.45
		Temporal	−0.06	(−0.07, −0.05)	<0.001	−0.06	(−0.07, −0.04)	<0.001
		Occipital	0.05	(0.04, 0.07)	<0.001	0.05	(0.03, 0.06)	<0.001
		Cingulate	0.04	(0.02, 0.05)	<0.001	0.03	(0.02, 0.05)	<0.001
		Insula	−0.02	(−0.04, 0.00)	0.015	−0.02	(−0.04, 0.00)	0.075
	Subcortical volume (mm^3)	Thalamus	−192.7	(−263.1, −122.3)	<0.001	−184.0	(−255.4, −112.5)	<0.001
		Caudate	−34.4	(−91.2, 22.5)	0.24	−45.4	(−103.6, 12.8)	0.13
		Putamen	−46.2	(−107.3, 14.8)	0.14	−60.6	(−122.4, 1.3)	0.055
		Pallidum	−49.8	(−76.3, −23.2)	<0.001	−49.3	(−76.4,−22.1)	<0.001
		Hippocampus	−58.4	(−104.2, −12.7)	0.012	−55.4	(−101.6, −9.3)	0.019
		Amygdala	−38.9	(−62.0, −15.8)	0.001	−36.2	(−59.7, −12.6)	0.003
		Nucleus accumbens	−63.1	(−76.2, −50.0)	<0.001	−56.8	(−70.1, −43.5)	<0.001
PM2.5	Cortical thickness (mm)	Global	0.01	(−0.05, 0.08)	0.67	0.01	(−0.06, 0.08)	0.87
		Frontal	−0.03	(−0.11, 0.06)	0.51	−0.03	(−0.12, 0.05)	0.46
		Parietal	0.02	(−0.07, 0.11)	0.62	0.00	(−0.08, 0.09)	0.95
		Temporal	−0.20	(−0.29, −0.11)	<0.001	−0.18	(−0.27, −0.08)	<0.001
		Occipital	0.21	(0.11, 0.31)	<0.001	0.16	(0.06, 0.26)	0.002
		Cingulate	0.18	(0.07, 0.28)	0.001	0.15	(0.04, 0.26)	0.007
		Insula	−0.09	(−0.22, 0.03)	0.14	−0.07	(−0.2, 0.06)	0.28
	Subcortical volume (mm^3)	Thalamus	−486.5	(−961.9,−11.1)	0.045	−541.9	(−1,020.8, −63.0)	0.027
		Caudate	−208.1	(−586.9, 170.8)	0.28	−267.8	(−653.9, 118.4)	0.18
		Putamen	−186.5	(−593.5, 220.6)	0.37	−300.8	(−711.4, 109.9)	0.15
		Pallidum	−156.3	(−334.2, 21.6)	0.085	−169.7	(−350.7, 11.4)	0.067
		Hippocampus	−145.9	(−451.6, 159.7)	0.35	−222.0	(−528.4, 84.4)	0.16
		Amygdala	−102.6	(−257.4, 52.3)	0.20	−110.8	(−267.7, 46.0)	0.17
		Nucleus accumbens	−239.0	(−329.0, −149.0)	<0.001	−203.3	(−293.7, −112.9)	<0.001
NO_2	Cortical thickness (mm)	Global	−0.01	(−0.01, 0.00)	0.001	−0.01	(−0.01, 0.00)	0.002
		Frontal	−0.02	(−0.03, −0.02)	<0.001	−0.02	(−0.03, −0.01)	<0.001
		Parietal	−0.02	(−0.03, −0.01)	<0.001	−0.02	(−0.03, −0.01)	<0.001
		Temporal	−0.04	(−0.05, −0.04)	<0.001	−0.04	(−0.05, −0.03)	<0.001
		Occipital	0.02	(0.01, 0.03)	<0.001	0.02	(0.01, 0.03)	<0.001
		Cingulate	0.03	(0.02, 0.03)	<0.001	0.03	(0.02, 0.03)	<0.001
		Insula	−0.02	(−0.03, −0.01)	0.002	−0.01	(−0.02, 0.00)	0.005
	Subcortical volume (mm^3)	Thalamus	−128.1	(−164.9, −91.3)	<0.001	−129.1	(−166.6,−91.5)	<0.001
		Caudate	−32.0	(−61.9, −2.0)	0.037	−38.3	(−69.2, −7.5)	0.015
		Putamen	5.5	(−26.8, 37.7)	0.74	−7.1	(−40.1, 25.8)	0.67
		Pallidum	−23.9	(−37.9, −9.9)	0.001	−26.2	(−40.7, −11.8)	<0.001
		Hippocampus	− 5.1	(−29.3, 19.2)	0.68	−7.2	(−31.7, 17.4)	0.57
		Amygdala	−24.1	(−36.3, −11.9)	<0.001	−23.8	(−36.3, −11.3)	<0.001
		Nucleus accumbens	−28.7	(−35.7, −21.7)	<0.001	−28.2	(−35.2, −21.1)	<0.001

Note: Beta coefficients (per 10-unit increase in each pollutant) were from generalized linear models. Model 1 was adjusted for age, sex, education level, marital status, income, survey year, and intracranial volume. Model 2 was adjusted for the Model 1 variables plus body mass index; smoking; alcohol consumption; walking days per week; history of hypertension, diabetes, hyperlipidemia, and angina or myocardial infarction; systolic blood pressure; diastolic blood pressure; fasting blood glucose level; and total cholesterol level. CI, confidence interval; NO_2, nitrogen dioxide; PM, particulate matter; PM2.5, PM ≤2.5 μm in aerodynamic diameter; PM10, PM ≤10 μm in aerodynamic diameter.

S2. None of the included covariates significantly differed between the two groups.

Association between Air Pollution and Brain Imaging Markers

Cortical thickness. A 10-$\mu g/m^3$ increase in PM10 was significantly associated with thinner frontal {–0.02 mm [95% confidence interval (CI): –0.03, –0.01] and temporal cortices [–0.06 mm (95% CI: –0.07, –0.05)] (Model 2 estimates; Table 2). PM10 was also significantly associated with increased occipital [0.05 mm (95% CI: 0.04, 0.07)] and cingulate thicknesses [0.03 mm (95% CI: 0.02, 0.05)]. A 10-$\mu g/m^3$ increase in PM2.5 was significantly associated with a thinner temporal cortex [–0.18 mm (95% CI: –0.27, –0.08)]. PM2.5 was also significantly associated with increased occipital [0.15 mm (95% CI: 0.06, 0.26)] and cingulate thicknesses [0.15 mm (95% CI: 0.04, 0.26)]. A 10-ppb increase in NO_2 was significantly associated with thinner global [–0.01 mm (95% CI: –0.01, 0.00)], frontal [–0.02 mm (95% CI: –0.03, –0.01)], parietal [–0.02 mm (95% CI: –0.03, –0.01)], temporal [–0.04 mm (95% CI: –0.05,–0.03)], and insular thicknesses [–0.01 mm (95% CI: –0.02, 0.00)]. NO_2 was also significantly associated with increased occipital [0.02 mm (95% CI: 0.01, 0.03)] and cingulate thicknesses [0.03 mm (95% CI: 0.02, 0.03)].

Subcortical volume. A 10-$\mu g/m^3$ increase in PM10 was significantly associated with reduced volumes of the thalamus [–184.0 mm^3 (95% CI: –255.4, –112.5)], pallidum [–49.3 mm^3 (95% CI: –76.4, –22.1)], hippocampus [–55.4 mm^3 (95% CI: –101.6, –9.3)], amygdala [–36.2 mm^3 (95% CI: –59.7, –12.6)], and nucleus accumbens [–56.8 mm^3 (95% CI: –70.1, –43.5)] (Model 2 estimates; Table 2). A 10-$\mu g/m^3$ increase in PM2.5 was significantly associated with reduced volumes of the thalamus [–541.9 mm^3 (95% CI: –1,020.8, –63.0)] and nucleus accumbens [–203.3 mm^3 (95% CI: –293.7, –112.9)]. A 10-ppb increase in NO_2 was significantly associated with reduced volumes of the thalamus [–129.1 mm^3 (95% CI: –166.6, –91.5)], caudate [–38.3 mm^3 (95% CI: –69.2, –7.5)], pallidum [–26.2 mm^3 (95% CI: –40.7, –11.8)], amygdala [–23.8 mm^3 (95% CI: –36.3, –11.3)], and nucleus accumbens [–28.2 mm^3 (95% CI: –35.2, –21.1)].

Sex difference. Associations between PM10 and global cortical thickness differed significantly between men and women [–0.02 mm (95% CI; –0.04, 0.00) in men vs. 0.01 mm (95% CI:

Table 3. Sex difference in the association between air pollution and brain imaging markers (Model 2).

			Men ($n = 427$)		Women ($n = 530$)		
Pollutant	Measurement	Brain region	Beta	(95% CI)	Beta	(95% CI)	$p_{interaction}$
PM10	Cortical thickness (mm)	Global	−0.02	(−0.04, 0.00)	0.01	(0.00, 0.02)	0.034
		Frontal	−0.03	(−0.05, −0.01)	−0.01	(−0.02, 0.01)	0.16
		Parietal	−0.02	(−0.04, 0.00)	0.01	(−0.01, 0.02)	0.034
		Temporal	−0.08	(−0.10, −0.06)	−0.04	(−0.05, −0.02)	0.005
		Occipital	0.03	(0.01, 0.05)	0.06	(0.03, 0.08)	0.034
		Cingulate	0.03	(0.00, 0.05)	0.03	(0.01, 0.05)	1.00
		Insula	−0.04	(−0.07, −0.01)	0.01	(−0.02, 0.03)	0.025
	Subcortical volume (mm^3)	Thalamus	−259.8	(−381.9, −137.7)	−108.3	(−195.1, −21.4)	0.047
		Caudate	−17.4	(−110.2, 75.3)	−68.8	(−144.7, 7.2)	0.40
		Putamen	−58.0	(−157.7, 41.7)	−63.6	(−144.2, 16.9)	0.93
		Pallidum	−29.1	(−70.0, 11.7)	−61.3	(−98.8, −23.9)	0.25
		Hippocampus	−106.9	(−179.9, −33.9)	−24.4	(−83.6, 34.9)	0.086
		Amygdala	−51.2	(−90.0, −12.4)	−26.0	(−56.1, 4.1)	0.32
		Nucleus accumbens	−62.0	(−82.3, −41.7)	−49.3	(−66.9, −31.6)	0.35
PM2.5	Cortical thickness (mm)	Global	−0.06	(−0.17, 0.05)	0.07	(−0.02, 0.16)	0.096
		Frontal	−0.12	(−0.25, 0.01)	0.05	(−0.06, 0.16)	0.065
		Parietal	−0.04	(−0.18, 0.1)	0.04	(−0.08, 0.15)	0.39
		Temporal	−0.32	(−0.46, −0.17)	−0.04	(−0.17, 0.08)	0.002
		Occipital	0.15	(0.00, 0.03)	0.16	(0.02, 0.3)	0.92
		Cingulate	0.14	(−0.03, 0.31)	0.15	(0.01, 0.29)	0.93
		Insula	−0.18	(−0.39, 0.02)	0.05	(−0.11, 0.21)	0.072
	Subcortical volume (mm^3)	Thalamus	−827.0	(−1,657.6, 3.6)	−245.6	(−810.9, 319.7)	0.26
		Caudate	−220.6	(−840.9, 399.7)	−257.7	(−750.4, 235)	0.93
		Putamen	−357.0	(−1,024.2, 310.2)	−253.4	(−775.5, 268.7)	0.81
		Pallidum	−124.6	(−398.2, 149.1)	−193.8	(−438.2, 50.7)	0.71
		Hippocampus	−218.4	(−711.3, 274.6)	−255.6	(−638.7, 127.5)	0.91
		Amygdala	−154.7	(−415.8, 106.4)	−77.3	(−272.5, 118)	0.64
		Nucleus accumbens	−278.3	(−417.5, −139.1)	−111.7	(−228.9, 5.6)	0.073
NO_2	Cortical thickness (mm)	Global	−0.01	(−0.02, −0.01)	0.00	(−0.01, 0.01)	1.00
		Frontal	−0.03	(−0.03, −0.02)	−0.01	(−0.02, 0.00)	0.16
		Parietal	−0.02	(−0.03, −0.01)	−0.01	(−0.02, 0.00)	0.48
		Temporal	−0.05	(−0.06, −0.04)	−0.03	(−0.04, −0.02)	0.16
		Occipital	0.01	(0.00, 0.02)	0.02	(0.01, 0.04)	0.48
		Cingulate	0.02	(0.01, 0.04)	0.02	(0.01, 0.04)	1.00
		Insula	−0.02	(−0.04, −0.01)	0.00	(−0.01, 0.02)	0.16
	Subcortical volume (mm^3)	Thalamus	−154.7	(−216.3, −93.0)	−96.9	(−148.7, −45.1)	0.16
		Caudate	−44.1	(−91.1, 2.9)	−41.1	(−86.8, 4.5)	0.93
		Putamen	−6.3	(−57.1, 44.5)	−16.7	(−65.1, 31.8)	0.77
		Pallidum	−12.4	(−33.2, 8.4)	−40.6	(−63.0, −18.1)	0.071
		Hippocampus	−25.8	(−63.2, 11.7)	−14.1	(−49.7, 21.5)	0.66
		Amygdala	−34.4	(−54, −14.7)	−20.5	(−38.6, −2.5)	0.31
		Nucleus accumbens	−32.5	(−42.8, −22.2)	−18.4	(−29.2, −7.6)	0.065

Note: Beta coefficients (per 10-unit increase in each pollutant) were from generalized linear models, adjusted for age; education level; marital status; income; body mass index; smoking; alcohol consumption; walking days per week; history of hypertension, diabetes, hyperlipidemia, and angina or myocardial infarction; systolic blood pressure; diastolic blood pressure; fasting blood glucose level; total cholesterol level; survey year; and intracranial volume. CI, confidence interval; NO_2, nitrogen dioxide; PM, particulate matter; PM2.5, PM ≤2.5 μm in aerodynamic diameter; PM10, PM ≤10 μm in aerodynamic diameter.

0.00, 0.02) in women; $p_{interaction} = 0.03$] (Model 2 estimates; Table 3). Significant differences with a similar pattern of inverse associations in men and weak positive associations in women were also evident for the parietal and insular lobes, whereas associations were inverse in both groups but stronger in men than women for the temporal lobe. Significant differences between men and women were also estimated for positive associations between PM10 and occipital thickness, with a weaker association in men than women [0.03 mm (95% CI: 0.01, 0.05) and 0.06 mm (95% CI: 0.03, 0.08), respectively, $p_{interaction} = 0.03$]. The association between PM10 and a smaller subcortical volume was significantly stronger in men [–259.8 mm^3 (95% CI: –318.9, –137.7)] than women [–108.3 mm^3 (95% CI: –195.1, –21.4)] ($p_{interaction} = 0.047$). Otherwise, associations between PM10 and subcortical volumes were similar between men and women ($p_{interaction} = 0.09$–0.93). Associations between PM2.5 and cortical thickness were inverse in both groups but much stronger in men [–0.32 mm (95% CI: –0.46, –0.17)] than women [–0.04 mm (95% CI: –0.17, 0.08)] for the temporal lobe ($p_{interaction} = 0.002$). Otherwise, associations between PM2.5 and brain imaging markers were similar between men and women ($p_{interaction} = 0.065$–0.93). Associations between NO_2 and brain imaging markers did not differ significantly between men and women. Model 1 estimates are presented in Table S3.

Association between Air Pollution and Brain Imaging Markers after PSM

ROI-based analysis. The higher (vs. lower) PM10 group had significantly thinner frontal [−0.02 mm (95% CI: –0.03, 0.00)] and temporal cortices [−0.06 mm (95% CI: –0.08, –0.04)] and significantly thicker occipital [0.05 mm (95% CI: 0.03, 0.07)] and cingulate cortices [0.02 mm (95% CI: 0.01, 0.04)] (Table 4). The higher (vs. lower) PM2.5 group had significantly thinner frontal [−0.02 mm (95% CI: –0.04, 0.00)] and temporal cortices [−0.05 mm (95% CI: –0.06, –0.03)] and significantly thicker occipital [0.04 mm (95% CI: 0.02, 0.06)] and cingulate cortices [0.03 mm (95% CI: 0.00, 0.05)]. The higher (vs. lower) NO_2 group had a significantly thinner temporal cortex [−0.05 mm (95% CI: –0.07, –0.03)] and significantly thicker occipital [0.03 mm (95% CI: 0.01, 0.05)] and cingulate cortices [0.04 mm (95% CI: 0.02, 0.06)]. The higher PM10 group had significantly

Table 4. Association between air pollution and brain magnetic resonance imaging markers in propensity score-matched individuals.

Pollutant	Measurement	Brain region	Beta	(95% CI)	*p*-Value
PM10	Cortical thickness (mm)	Global	−0.01	(−0.02, 0.01)	0.27
		Frontal	−0.02	(−0.03, 0.00)	0.044
		Parietal	−0.01	(−0.03, 0.01)	0.27
		Temporal	−0.06	(−0.08, −0.04)	<0.001
		Occipital	0.05	(0.03, 0.07)	<0.001
		Cingulate	0.02	(0.01, 0.04)	0.006
		Insula	−0.01	(−0.03, 0.01)	0.27
	Subcortical volume (mm^3)	Thalamus	−215.2	(−307.7, −122.6)	<0.001
		Caudate	−47.5	(−112.4, 17.5)	0.15
		Putamen	−34.0	(−111.8, 43.7)	0.39
		Pallidum	−65.2	(−96.4, −34.0)	<0.001
		Hippocampus	−85.8	(−143.0, −28.7)	0.004
		Amygdala	−42.4	(−73.3, −11.4)	0.008
		Nucleus accumbens	−65.2	(−81.2, −49.1)	<0.001
PM2.5	Cortical thickness (mm)	Global	0.00	(−0.02, 0.01)	0.62
		Frontal	−0.02	(−0.04, 0.00)	0.033
		Parietal	0.00	(−0.02, 0.01)	0.70
		Temporal	−0.05	(−0.06, −0.03)	<0.001
		Occipital	0.04	(0.02, 0.06)	<0.001
		Cingulate	0.03	(0.00, 0.05)	0.016
		Insula	0.00	(−0.02, 0.01)	0.70
	Subcortical volume (mm^3)	Thalamus	−78.7	(−173.7, 16.2)	0.11
		Caudate	−14.2	(−81.8, 53.5)	0.68
		Putamen	−2.0	(−79.8, 75.8)	0.96
		Pallidum	−1.1	(−33.5, 31.4)	0.95
		Hippocampus	−30.2	(−89.2, 28.7)	0.32
		Amygdala	−25.2	(−53.3, 2.9)	0.08
		Nucleus accumbens	−52.8	(−68.4, −37.1)	<0.001
NO_2	Cortical thickness (mm)	Global	0.00	(−0.01, 0.02)	0.89
		Frontal	−0.02	(−0.03, 0.00)	0.12
		Parietal	−0.01	(−0.03, 0.01)	0.18
		Temporal	−0.05	(−0.07, −0.03)	<0.001
		Occipital	0.03	(0.01, 0.05)	0.002
		Cingulate	0.04	(0.02, 0.06)	<0.001
		Insula	−0.01	(−0.03, 0.01)	0.18
	Subcortical volume (mm^3)	Thalamus	−211.5	(−317.6, −105.3)	<0.001
		Caudate	−113.6	(−179.9, −47.4)	0.001
		Putamen	−17.9	(−98.9, 63.0)	0.67
		Pallidum	−45.6	(−80.2, −10.9)	0.011
		Hippocampus	−32.2	(−99.5, 35.0)	0.35
		Amygdala	−23.6	(−56.2, 9.1)	0.16
		Nucleus accumbens	−48.4	(−66.4, −30.3)	<0.001

Note: Beta coefficients were from linear mixed models including 66.6 percentile or higher (vs. 33.3 percentile or lower) air pollution and intracranial volume, with a matched pair as a random effect. CI, confidence interval; NO_2, nitrogen dioxide; PM, particulate matter; PM2.5, PM ≤2.5 μm in aerodynamic diameter; PM10, PM ≤10 μm in aerodynamic diameter.

reduced volumes of the thalamus, pallidum, hippocampus, amygdala, and nucleus accumbens. The higher PM2.5 groups had a significantly reduced volume in the nucleus accumbens. The higher NO_2 group had significantly reduced volumes of the thalamus, caudate, pallidum, and nucleus accumbens.

Surface-based morphometry. In SBM with FDR correction, thinner brain regions in the higher (vs. lower) PM10 group included the bilateral lateral temporal cortices, inferior parietal cortices, prefrontal cortices, posterior cingulate cortices, insular cortices, parahippocampal gyri, and fusiform gyri (Figure 1A). Thicker brain regions in the higher PM10 group were the bilateral occipital cortices and postcentral gyri. The higher (vs. lower) PM2.5 group had reduced thicknesses in the bilateral lateral temporal cortices, inferior parietal cortices, prefrontal cortices, insular cortices, parahippocampal gyri, and fusiform gyri (Figure 1B). The higher PM2.5 group also had increased thicknesses in the bilateral occipital cortices and postcentral gyri. The higher (vs. lower) NO_2 group had reduced thicknesses in the bilateral frontal cortices, lateral temporal cortices, inferior parietal cortices, posterior cingulate cortices, insular cortices, parahippocampal gyri, and fusiform gyri (Figure 1C). The higher NO_2 group also had increased thicknesses in the bilateral occipital cortices and left postcentral gyrus.

In SBM with cluster-wise correction, the higher (vs. lower) PM10 group had reduced thicknesses in the bilateral lateral temporal cortices, bilateral posterior cingulate cortices, left fusiform gyrus, right supramarginal gyrus, and right parahippocampal gyrus (Figure S1A). The higher PM10 groups also had increased thickness in the bilateral lingual gyri, left lateral occipital gyrus, right pericalcarine, and right cuneus. Thinner brain regions in the higher (vs. lower) PM2.5 group included the bilateral lateral temporal cortices, left supramarginal cortex, and left fusiform gyrus (Figure S1B). Thicker brain regions in the higher PM2.5 group were the bilateral lateral occipital cortices and lingual gyri. The higher (vs. lower) NO_2 group had reduced thicknesses in the bilateral lateral temporal cortices, bilateral inferior parietal cortices, bilateral frontal cortices, bilateral fusiform gyri, left cuneus, and right parahippocampal gyrus (Figure S1C). The higher NO_2 group also had increased thicknesses in the bilateral lateral occipital cortices.

Two-Pollutant Models

After adjusting for NO_2, the inverse association between PM10 and temporal thickness was null, whereas the positive association between PM10 and occipital thickness persisted (Table 5). After adjusting for NO_2, the inverse association between PM2.5 and

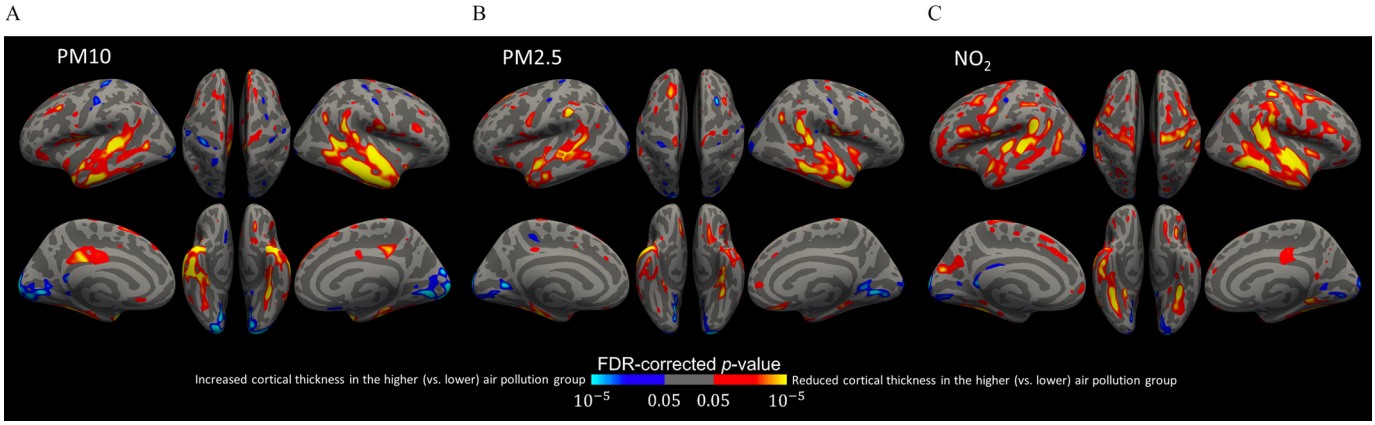

Figure 1. Brain regions associated with (A) PM10, (B) PM2.5, and (C) NO_2 in surface-based morphometry [with false discovery rate (FDR) correction for multiple comparisons]. Paired *t*-tests were performed on every vertex of the reference surface between propensity score-matched groups (the higher and lower air pollution groups), with FDR correction for multiple comparisons ($p < 0.05$). The red color indicates the brain regions with reduced cortical thickness and the blue color indicates those with increased cortical thickness in the higher (vs. lower) air pollution group. Note: NO_2, nitrogen dioxide; PM, particulate matter; PM2.5, PM $\leq$2.5 μm in aerodynamic diameter; PM10, PM $\leq$10 μm in aerodynamic diameter.

temporal thickness and the positive associations of PM2.5 with occipital and insular thicknesses were null. By contrast, the inverse associations between NO_2 and cortical thickness in the global, frontal, parietal, temporal, and insular lobes were comparable in magnitude before and after adjustment of PM10 or PM2.5. After adjusting for PM10, the positive association of NO_2 with cingulate thickness persisted, whereas the positive association with occipital thickness was null. After adjusting for PM2.5, the positive associations of NO_2 with cingulate and occipital thicknesses persisted.

Sensitivity Analyses

In the sensitivity analysis constrained to participants without possible cognitive impairment, the directions and magnitudes of all the associations were similar to those in the main analysis (Table S4). In the sensitivity analysis constrained to participants who underwent the survey from 2015, the inverse association between PM2.5 and temporal thickness and the positive associations of PM2.5 with occipital and cingulate thicknesses were stronger than in the main analysis (Table S5). The inverse associations between PM2.5 and reduced volumes of the thalamus and nucleus accumbens were also stronger than in the main analysis.

Discussion

We investigated associations of ambient air pollutants with cortical thickness and subcortical volume in adults. The main finding was that all the studied pollutants (i.e., PM10, PM2.5, and NO_2) were associated with a reduced cortical thickness in the temporal lobe. PM10 was associated with a reduced thickness in the frontal lobe as well, and NO_2 was associated with reduced thicknesses in more extensive areas (global, frontal, parietal, temporal, and insular lobes). Positive associations between all the studied pollutants and cortical thickness in the occipital and cingulate lobes were also found. In addition, all the studied pollutants were associated with reduced volumes of the thalamus and nucleus accumbens.

The temporal lobe was most strongly associated with the air pollutants in the main analysis as well as in the ROI-based and SBM analyses after PSM. The ROI-based analysis of the Women's Health Initiative Memory Study (WHIMS)–MRI cohort revealed a significant association between exposure to PM2.5 and decreased white matter volume in the temporal lobe, but not with gray matter volume (Chen et al. 2015). Other studies have shown null associations between air pollution and gray matter volume in the temporal lobe (Casanova et al. 2016; Chen et al. 2015; Power et al. 2018). This discrepancy might reflect noncausal sources of variation among the studies (e.g., residual confounding, selection bias, random error), but the present study used brain cortical thickness, a more sensitive indicator of brain structural changes (Burggren et al. 2008; Thambisetty et al. 2010); thus, we may have detected pollution-induced changes that occurred earlier than volumetric changes. Furthermore, we found that an increase in PM10 was significantly associated with reduced volumes of the hippocampus and amygdala in the main analysis and the post hoc ROI-based analysis after PSM. Although previous epidemiological studies have reported null associations between PM2.5 and hippocampal volumes (Casanova et al. 2016; Chen et al. 2015; Power et al. 2018; Wilker et al. 2015), an animal study showed that PM administration induced synaptic function impairment, which is related to reduced gray matter volumes (Fjell and Walhovd 2010), in the mouse hippocampus (Davis et al. 2013). Taken together with studies suggesting reduced hippocampal and amygdala volumes in cognitively impaired individuals (Shi et al. 2009; Zanchi et al. 2017), it is possible that air pollution exposure affects the hippocampus and amygdala, leading to cognitive decline.

The frontal lobe exhibited significant cortical thinning associated with PM10 and NO_2 in the main analysis. After PSM, the higher PM10 or PM2.5 group had significantly reduced frontal thicknesses in the ROI-based analysis and SBM with FDR correction. These findings align with a substantial number of studies linking air pollution to reduced memory function (Ailshire and Crimmins 2014; Kulick et al. 2020a, 2020b; Petkus et al. 2020; Tonne et al. 2014; Weuve et al. 2012; Wurth et al. 2018; Younan et al. 2020) given that the frontal lobe is related to working and episodic memory. However, the previous neuroimaging study findings are conflicting. The voxel-based WHIMS-MRI analysis showed that PM2.5 was primarily associated with the dorsolateral and medial prefrontal cortex (Casanova et al. 2016). Conversely, the ROI-based ARIC analysis reported null associations between exposure to PM10 and PM2.5 and frontal volumes (Power et al. 2018). In addition to noncausal sources of variation among the studies, the discrepancy may be attributable to differences in proportions of PM constituents across geographical regions. PM is a mixture of a range of pollutants (e.g., sulfur oxides, nitrogen oxides, heavy metals, hydrocarbons) and these constituents might be individually linked to brain structures given that our recent study demonstrated the association between polycyclic aromatic hydrocarbons and brain cortical thinning in adults (Cho et al. 2020). Future studies are warranted to explore the associations between PM constituents and brain MRI markers.

Table 5. Association between air pollution and brain magnetic resonance imaging markers based on two-pollutant models.

Pollutant	Measurement	Brain region	Beta	(95% CI)	*p*-Value
PM10 (adjusted for NO_2)	Cortical thickness (mm)	Global	0.01	(0.00, 0.03)	0.055
		Frontal	0.01	(0.00, 0.03)	0.094
		Parietal	0.03	(0.01, 0.05)	<0.001
		Temporal	−0.01	(−0.03, 0.01)	0.30
		Occipital	0.04	(0.02, 0.06)	<0.001
		Cingulate	0.00	(−0.02, 0.03)	0.68
		Insula	0.00	(−0.02, 0.03)	0.95
	Subcortical volume (mm^3)	Thalamus	−45.2	(−138.2, 47.9)	0.34
		Caudate	2.6	(−73.9, 79.1)	0.95
		Putamen	−89.7	(−171.1, −8.3)	0.031
		Pallidum	−29.7	(−65.4, 6)	0.10
		Hippocampus	−80.8	(−141.5, −20.1)	0.009
		Amygdala	−12.2	(−43.1, 18.7)	0.44
		Nucleus accumbens	−38.7	(−56.1, −21.3)	<0.001
PM2.5 (adjusted for NO_2)	Cortical thickness (mm)	Global	0.05	(−0.02, 0.13)	0.15
		Frontal	0.08	(−0.01, 0.17)	0.075
		Parietal	0.11	(0.01, 0.20)	0.026
		Temporal	0.02	(−0.08, 0.11)	0.71
		Occipital	0.09	(−0.02, 0.20)	0.097
		Cingulate	0.04	(−0.08, 0.15)	0.54
		Insula	0.00	(−0.14, 0.13)	0.98
	Subcortical volume (mm^3)	Thalamus	76.9	(−429.6, 583.4)	0.77
		Caudate	−101.7	(−517.9, 314.6)	0.63
		Putamen	−311.5	(−755.2, 132.2)	0.17
		Pallidum	−53.8	(−248.4, 140.9)	0.59
		Hippocampus	−219.5	(−550.6, 111.6)	0.19
		Amygdala	1.4	(−167, 169.7)	0.99
		Nucleus accumbens	−82.4	(−177.9, 13)	0.091
NO_2 (adjusted for PM10)	Cortical thickness (mm)	Global	−0.01	(−0.02, −0.01)	<0.001
		Frontal	−0.03	(−0.03, −0.02)	<0.001
		Parietal	−0.03	(−0.04, −0.02)	<0.001
		Temporal	−0.04	(−0.05, −0.03)	<0.001
		Occipital	0.00	(−0.01, 0.01)	0.51
		Cingulate	0.02	(0.01, 0.03)	<0.001
		Insula	−0.01	(−0.03, 0.00)	0.028
	Subcortical volume (mm^3)	Thalamus	−113.5	(−162.9, −64.1)	<0.001
		Caudate	−39.2	(−79.9, 1.4)	0.059
		Putamen	23.8	(−19.4, 67.1)	0.28
		Pallidum	−16.0	(−34.9, 3)	0.099
		Hippocampus	20.7	(−11.5, 53)	0.21
		Amygdala	−19.6	(−36, −3.1)	0.02
		Nucleus accumbens	−14.8	(−24, −5.6)	0.002
NO_2 (adjusted for PM2.5)	Cortical thickness (mm)	Global	−0.01	(−0.02, 0.00)	0.001
		Frontal	−0.02	(−0.03, −0.02)	<0.001
		Parietal	−0.02	(−0.03, −0.01)	<0.001
		Temporal	−0.04	(−0.05,−0.03)	<0.001
		Occipital	0.01	(0.01, 0.02)	0.001
		Cingulate	0.02	(0.01, 0.03)	<0.001
		Insula	−0.01	(−0.03, 0.00)	0.009
	Subcortical volume (mm^3)	Thalamus	−131.4	(−172, −90.8)	<0.001
		Caudate	−35.3	(−68.6, −1.9)	0.039
		Putamen	2.3	(−33.3, 37.8)	0.90
		Pallidum	−24.6	(−40.2, −9)	0.002
		Hippocampus	−0.5	(−27.1, 26)	0.97
		Amygdala	−23.8	(−37.3, −10.3)	0.001
		Nucleus accumbens	−25.7	(−33.3,−18)	<0.001

Note: Beta coefficients (per 10-unit increase in each pollutant) were from generalized linear models, adjusted for age; sex; education level; marital status; income; body mass index; smoking; alcohol consumption; walking days per week; history of hypertension, diabetes, hyperlipidemia, and angina or myocardial infarction; systolic blood pressure; diastolic blood pressure; fasting blood glucose level; total cholesterol level; survey year; and intracranial volume. CI, confidence interval; NO_2, nitrogen dioxide; PM, particulate matter; PM2.5, PM ≤2.5 μm in aerodynamic diameter; PM10, PM ≤10 μm in aerodynamic diameter.

We also found associations between pollutants and reduced volumes of the thalamus (PM10, PM2.5, and NO_2), caudate (NO_2 only), and pallidum (PM10 and NO_2), which is in accord with the ARIC analysis showing reduced thalamus, caudate, putamen, and pallidum volumes related to PM10 (Power et al. 2018). Conversely, the voxel-based WHIMS-MRI analysis reported increased deep gray matter volume related to PM2.5 (Casanova et al. 2016). Little is known about the positive association between PM2.5 and deep gray matter volume. To determine the reason for the opposing associations, it may be necessary to dissect each subcortical structure from deep gray matter when measuring cortical volume. In the present study, the nucleus accumbens was likewise inversely associated with air pollution. This finding is supported by animal studies demonstrating dopaminergic neuron loss induced by PM in the striatum (caudate, putamen, and nucleus accumbens) (Gillespie et al. 2013; Veronesi et al. 2005). Further, given that the nucleus accumbens is a subcortical structure related to rewards and addictive behaviors, the finding is in accord with a previous study showing the positive associations of PM and NO_2 with substance abuse (Szyszkowicz et al. 2018).

Unexpectedly, the studied air pollutants were positively associated with occipital and cingulate thicknesses in most of the analyses. Previous studies have reported mixed findings on the association between PM and the occipital lobe (Casanova et al. 2016; Power et al. 2018). The ARIC analysis, which included four U.S. sites, found an inverse association between PM10 and occipital volume in Minnesota as well as a positive association between PM2.5 and occipital volume in Mississippi (Power et al. 2018). The voxel-based analysis of the WHIMS-MRI cohort demonstrated an inverse association between PM2.5 and occipital poles (Casanova et al. 2016). The occipital lobe is the primary visual cortex and is known to be less important in the pathophysiology of Alzheimer's disease (the most common form of dementia) as compared with the frontal and temporal lobes (Miller and Boeve 2016). More studies are required to investigate whether air pollution has divergent effects on different cortices of the human brain.

There were several notable strengths of the present study. First, nearly 1,000 individuals were included, which is a relatively large sample for neuroimaging studies. Although two different MRI scanners were involved, we used the same protocol and accounted for potential variation. Second, higher-resolution MRI scanners were used compared with prior studies (Casanova et al. 2016; Chen et al. 2015; Pujol et al. 2016a, 2016b). Last, we conducted SBM as a complementary analysis to the ROI-based analysis of brain images. The ROI-based approach facilitated clinical interpretation by predefining brain regions, whereas SBM enabled the detection of potential small (and not predefined) brain regions associated with air pollution. Because the ROI-based analysis estimates mean values of predefined brain regions, there could be discrepancy in the results between the ROI-based analysis and SBM; specifically, a small region that shows significance in SBM might not be significant in the ROI-based analysis. Furthermore, we conducted both FDR correction and cluster-wise correction for multiple comparisons in SBM. Although cluster-wise correction yielded more conservative estimates, FDR correction enabled us to reduce the chances of missing an important hypothesis, aligning with the exploratory nature of the present study.

The study also had several limitations. First, the cross-sectional nature of our study might preclude suggesting temporal associations between air pollution exposure and brain MRI markers. To address this issue, we set the exposure window at 5 y (for PM10 and NO_2) and at 1 y (for PM2.5) prior to recruitment, and the median duration of residence was 15 y. Longitudinal investigations on brain MRI markers are needed to confirm the associations. Second, the present study may not be free from selection bias given that it included only individuals who underwent brain MRI scans. Although we invited participants to undergo brain MRI scans by order of enrollment, it is possible that the participants were more likely to have concerns about cognitive impairment and some of them had actual problem with memory. Third, there is a possibility of residual confounding by individual-level factors as well as contextual-level factors (e.g., neighborhood socioeconomic status, noise, greenness, population density). Fourth, the PM2.5 data were estimated based on monitoring that started in 2015. This means that there is temporal misalignment between brain MRI data and PM2.5 data in individuals who participated in the survey in 2014 ($n = 115$). However, this limitation may have led to the narrow range of PM2.5 concentrations and, hence, fewer significant associations between PM2.5 and brain regions. Long-term monitoring data are needed to obtain valid effect measures for the association between PM2.5 and brain MRI markers. Fifth, estimates based on Model 2 should be interpreted with caution given that the additional covariates may have included causal intermediates; albeit estimates from Model 2 were generally similar to those from Model 1. Last, small vessel diseases, such as white matter hyperintensities were not investigated on brain MRI. Although previous neuroimaging studies reported null associations between PM2.5 and white matter hyperintensities among the elderly (Wilker et al. 2015, 2016), future studies are needed to examine the mediation effect of white matter hyperintensities on associations between air pollution exposure and cortical thickness.

In conclusion, this study showed that long-term exposure to air pollution was associated with cortical thickness and subcortical volume in Korean adults without dementia, movement disorder, or stroke. An increase in PM or NO_2 concentrations was associated with reduced thicknesses in the frontal, temporal, parietal, and insular lobes, and with increased thicknesses in the occipital and cingulate lobes. An increase in PM or NO_2 concentrations was also associated with reduced volumes of the thalamus, caudate, pallidum, hippocampus, amygdala, and nucleus accumbens.

Acknowledgments

CK supervised and designed the study. J.C., Y.N., S.Y.K., J.S., J.N., W.K., S.-K.C., H.S., G.S., S.-K.L., S.-B.K., S.S.O., H.J.K., S.W.S., D.-S.S., and N.K. contributed to the data collection. J.C., Y.N., and S.S. analyzed the data. J.C., Y.N., S.Y.K., S.S., and C.K. drafted the manuscript. Y.N., S.Y.K., and C.K. provided significant intellectual input and a critical review of the manuscript. All authors approved the final version of the manuscript.

This research was supported by a grant from the Korea Ministry of Environment under the Environmental Health Action Program (2014001360002) and by grants from the Korea Health Technology R&D Project through the Korea Health Industry Development Institute, funded by the Ministry of Health and Welfare, Republic of Korea (HI18C1629 and HI14C1135).

References

Ailshire JA, Crimmins EM. 2014. Fine particulate matter air pollution and cognitive function among older US adults. Am J Epidemiol 180(4):359–366, PMID: 24966214, https://doi.org/10.1093/aje/kwu155.

Altman DG, Bland JM. 2003. Interaction revisited: the difference between two estimates. BMJ 326(7382):219, PMID: 12543843, https://doi.org/10.1136/bmj.326.7382.219.

Bind MA. 2019. Causal modeling in environmental health. Annu Rev Public Health 40:23–43, PMID: 30633715, https://doi.org/10.1146/annurev-publhealth-040218-044048.

Burggren AC, Zeineh MM, Ekstrom AD, Braskie MN, Thompson PM, Small GW, et al. 2008. Reduced cortical thickness in hippocampal subregions among cognitively normal apolipoprotein E e4 carriers. Neuroimage 41(4):1177–1183, PMID: 18486492, https://doi.org/10.1016/j.neuroimage.2008.03.039.

Casanova R, Wang X, Reyes J, Akita Y, Serre ML, Vizuete W, et al. 2016. A voxel-based morphometry study reveals local brain structural alterations associated with ambient fine particles in older women. Front Hum Neurosci 10:495, PMID: 27790103, https://doi.org/10.3389/fnhum.2016.00495.

Chen H, Kwong JC, Copes R, Hystad P, van Donkelaar A, Tu K, et al. 2017. Exposure to ambient air pollution and the incidence of dementia: a population-based cohort study. Environ Int 108:271–277, PMID: 28917207, https://doi.org/10.1016/j.envint.2017.08.020.

Chen JC, Wang X, Wellenius GA, Serre ML, Driscoll I, Casanova R, et al. 2015. Ambient air pollution and neurotoxicity on brain structure: evidence from Women's Health Initiative Memory Study. Ann Neurol 78(3):466–476, PMID: 26075655, https://doi.org/10.1002/ana.24460.

Cho J, Sohn J, Noh J, Jang H, Kim W, Cho SK, et al. 2020. Association between exposure to polycyclic aromatic hydrocarbons and brain cortical thinning: the Environmental Pollution-Induced Neurological EFfects (EPINEF) study. Sci Total Environ 737:140097, PMID: 32783831, https://doi.org/10.1016/j.scitotenv.2020.140097.

Cho Y, Seong JK, Jeong Y, Shin SY, Alzheimer's Disease Neuroimaging I. 2012. Individual subject classification for Alzheimer's disease based on incremental learning using a spatial frequency representation of cortical thickness data.

Neuroimage 59(3):2217–2230, PMID: 22008371, https://doi.org/10.1016/j.neuroimage.2011.09.085.
Dale AM, Fischl B, Sereno MI. 1999. Cortical surface-based analysis. I. Segmentation and surface reconstruction. Neuroimage 9(2):179–194, PMID: 9931268, https://doi.org/10.1006/nimg.1998.0395.
Davis DA, Akopian G, Walsh JP, Sioutas C, Morgan TE, Finch CE. 2013. Urban air pollutants reduce synaptic function of CA1 neurons via an NMDA/NÉ® pathway *in vitro*. J Neurochem 127(4):509–519, PMID: 23927064, https://doi.org/10.1111/jnc.12395.
Desikan RS, Ségonne F, Fischl B, Quinn BT, Dickerson BC, Blacker D, et al. 2006. An automated labeling system for subdividing the human cerebral cortex on MRI scans into gyral based regions of interest. Neuroimage 31(3):968–980, PMID: 16530430, https://doi.org/10.1016/j.neuroimage.2006.01.021.
Fischl B, Dale AM. 2000. Measuring the thickness of the human cerebral cortex from magnetic resonance images. Proc Natl Acad Sci USA 97(20):11050–11055, PMID: 10984517, https://doi.org/10.1073/pnas.200033797.
Fischl B, Salat DH, Busa E, Albert M, Dieterich M, Haselgrove C, et al. 2002. Whole brain segmentation: automated labeling of neuroanatomical structures in the human brain. Neuron 33(3):341–355, PMID: 11832223, https://doi.org/10.1016/s0896-6273(02)00569-x.
Fischl B, Salat DH, van der Kouwe AJ, Makris N, Ségonne F, Quinn BT, et al. 2004a. Sequence-independent segmentation of magnetic resonance images. Neuroimage 23(suppl 1):S69–S84, PMID: 15501102, https://doi.org/10.1016/j.neuroimage.2004.07.016.
Fischl B, Sereno MI, Dale AM. 1999a. Cortical surface-based analysis. II: inflation, flattening, and a surface-based coordinate system. Neuroimage 9(2):195–207, PMID: 9931269, https://doi.org/10.1006/nimg.1998.0396.
Fischl B, Sereno MI, Tootell RB, Dale AM. 1999b. High-resolution intersubject averaging and a coordinate system for the cortical surface. Hum Brain Mapp 8(4):272–284, PMID: 10619420, https://doi.org/10.1002/(SICI)1097-0193(1999)8:4<272::AID-HBM10>3.0.CO;2-4.
Fischl B, van der Kouwe A, Destrieux C, Halgren E, Ségonne F, Salat DH, et al. 2004b. Automatically parcellating the human cerebral cortex. Cereb Cortex 14(1):11–22, PMID: 14654453, https://doi.org/10.1093/cercor/bhg087.
Fjell AM, Walhovd KB. 2010. Structural brain changes in aging: courses, causes and cognitive consequences. Rev Neurosci 21(3):187–221, PMID: 20879692, https://doi.org/10.1515/revneuro.2010.21.3.187.
Gillespie P, Tajuba J, Lippmann M, Chen LC, Veronesi B. 2013. Particulate matter neurotoxicity in culture is size-dependent. Neurotoxicology 36:112–117, PMID: 22057156, https://doi.org/10.1016/j.neuro.2011.10.006.
Hagler DJ Jr, Saygin AP, Sereno MI. 2006. Smoothing and cluster thresholding for cortical surface-based group analysis of fMRI data. Neuroimage 33(4):1093–1103, PMID: 17011792, https://doi.org/10.1016/j.neuroimage.2006.07.036.
Hart JE, Yanosky JD, Puett RC, Ryan L, Dockery DW, Smith TJ, et al. 2009. Spatial modeling of PM_{10} and NO_2 in the continental United States, 1985–2000. Environ Health Perspect 117(11):1690–1696, PMID: 20049118, https://doi.org/10.1289/ehp.0900840.
Kim SY, Song I. 2017. National-scale exposure prediction for long-term concentrations of particulate matter and nitrogen dioxide in South Korea. Environ Pollut 226:21–29, PMID: 28399503, https://doi.org/10.1016/j.envpol.2017.03.056.
Kulick ER, Elkind MSV, Boehme AK, Joyce NR, Schupf N, Kaufman JD, et al. 2020a. Long-term exposure to ambient air pollution, APOE-ε4 status, and cognitive decline in a cohort of older adults in northern Manhattan. Environ Int 136:105440, PMID: 31926436, https://doi.org/10.1016/j.envint.2019.105440.
Kulick ER, Wellenius GA, Boehme AK, Joyce NR, Schupf N, Kaufman JD, et al. 2020b. Long-term exposure to air pollution and trajectories of cognitive decline among older adults. Neurology 94(17):e1782–e1792, PMID: 32269113, https://doi.org/10.1212/WNL.0000000000009314.
Kulick ER, Wellenius GA, Kaufman JD, DeRosa JT, Kinney PL, Cheung YK, et al. 2017. Long-term exposure to ambient air pollution and subclinical cerebrovascular disease in NOMAS (the Northern Manhattan Study). Stroke 48(7):1966–1968, PMID: 28455324, https://doi.org/10.1161/STROKEAHA.117.016672.
Miller BL, Boeve BF. 2016. *The Behavioral Neurology of Dementia*. Newark, NJ: Cambridge University Press.
Panizzon MS, Fennema-Notestine C, Eyler LT, Jernigan TL, Prom-Wormley E, Neale M, et al. 2009. Distinct genetic influences on cortical surface area and cortical thickness. Cereb Cortex 19(11):2728–2735, PMID: 19299253, https://doi.org/10.1093/cercor/bhp026.
Petkus AJ, Younan D, Widaman K, Gatz M, Manson JE, Wang X, et al. 2020. Exposure to fine particulate matter and temporal dynamics of episodic memory and depressive symptoms in older women. Environ Int 135:105196, PMID: 31881430, https://doi.org/10.1016/j.envint.2019.105196.
Power MC, Adar SD, Yanosky JD, Weuve J. 2016. Exposure to air pollution as a potential contributor to cognitive function, cognitive decline, brain imaging, and dementia: a systematic review of epidemiologic research. Neurotoxicology 56:235–253, PMID: 27328897, https://doi.org/10.1016/j.neuro.2016.06.004.
Power MC, Lamichhane AP, Liao D, Xu X, Jack CR, Gottesman RF, et al. 2018. The association of long-term exposure to particulate matter air pollution with brain MRI findings: the ARIC study. Environ Health Perspect 126(2):027009, PMID: 29467108, https://doi.org/10.1289/EHP2152.
Power MC, Weisskopf MG, Alexeeff SE, Coull BA, Spiro A III, Schwartz J. 2011. Traffic-related air pollution and cognitive function in a cohort of older men. Environ Health Perspect 119(5):682–687, PMID: 21172758, https://doi.org/10.1289/ehp.1002767.
Pujol J, Fenoll R, Maciá D, Martínez-Vilavella G, Alvarez-Pedrerol M, Rivas I, et al. 2016a. Airborne copper exposure in school environments associated with poorer motor performance and altered basal ganglia. Brain Behav 6(6):e00467, PMID: 27134768, https://doi.org/10.1002/brb3.467.
Pujol J, Martínez-Vilavella G, Maciá D, Fenoll R, Alvarez-Pedrerol M, Rivas I, et al. 2016b. Traffic pollution exposure is associated with altered brain connectivity in school children. Neuroimage 129:175–184, PMID: 26825441, https://doi.org/10.1016/j.neuroimage.2016.01.036.
Qiu A, Bitouk D, Miller MI. 2006. Smooth functional and structural maps on the neocortex via orthonormal bases of the Laplace-Beltrami operator. IEEE Trans Med Imaging 25(10):1296–1306, PMID: 17024833, https://doi.org/10.1109/tmi.2006.882143.
Ritchie SJ, Cox SR, Shen X, Lombardo MV, Reus LM, Alloza C, et al. 2018. Sex differences in the adult human brain: evidence from 5216 UK Biobank participants. Cereb Cortex 28(8):2959–2975, PMID: 29771288, https://doi.org/10.1093/cercor/bhy109.
Shi F, Liu B, Zhou Y, Yu C, Jiang T. 2009. Hippocampal volume and asymmetry in mild cognitive impairment and Alzheimer's disease: meta-analyses of MRI studies. Hippocampus 19(11):1055–1064, PMID: 19309039, https://doi.org/10.1002/hipo.20573.
Szyszkowicz M, Thomson EM, Colman I, Rowe BH. 2018. Ambient air pollution exposure and emergency department visits for substance abuse. PLoS One 13(6):e0199826, PMID: 29958279, https://doi.org/10.1371/journal.pone.0199826.
Thambisetty M, Wan J, Carass A, An Y, Prince JL, Resnick SM. 2010. Longitudinal changes in cortical thickness associated with normal aging. Neuroimage 52(4):1215–1223, PMID: 20441796, https://doi.org/10.1016/j.neuroimage.2010.04.258.
Tonne C, Elbaz A, Beevers S, Singh-Manoux A. 2014. Traffic-related air pollution in relation to cognitive function in older adults. Epidemiology 25(5):674–681, PMID: 25036434, https://doi.org/10.1097/EDE.0000000000000144.
Tzivian L, Dlugaj M, Winkler A, Weinmayr G, Hennig F, Fuks KB, et al. 2016. Long-term air pollution and traffic noise exposures and mild cognitive impairment in older adults: a cross-sectional analysis of the Heinz Nixdorf Recall study. Environ Health Perspect 124(9):1361–1368, PMID: 26863687, https://doi.org/10.1289/ehp.1509824.
Vallet B, Lévy B. 2008. Spectral geometry processing with manifold harmonics. Comput Graph Forum 27(2):251–260, https://doi.org/10.1111/j.1467-8659.2008.01122.x.
Veronesi B, Makwana O, Pooler M, Chen LC. 2005. Effects of subchronic exposures to concentrated ambient particles. VII. Degeneration of dopaminergic neurons in Apo $E^{-/-}$ mice. Inhal Toxicol 17(4–5):235–241, PMID: 15804941, https://doi.org/10.1080/08958370590912888.
Vienneau D, de Hoogh K, Beelen R, Fischer P, Hoek G, Briggs D. 2010. Comparison of land-use regression models between Great Britain and the Netherlands. Atmos Environ 44(5):688–696, https://doi.org/10.1016/j.atmosenv.2009.11.016.
Weuve J, Puett RC, Schwartz J, Yanosky JD, Laden F, Grodstein F. 2012. Exposure to particulate air pollution and cognitive decline in older women. Arch Intern Med 172(3):219–227, PMID: 22332151, https://doi.org/10.1001/archinternmed.2011.683.
Wilker EH, Martinez-Ramirez S, Kloog I, Schwartz J, Mostofsky E, Koutrakis P, et al. 2016. Fine particulate matter, residential proximity to major roads, and markers of small vessel disease in a memory study population. J Alzheimers Dis 53(4):1315–1323, PMID: 27372639, https://doi.org/10.3233/JAD-151143.
Wilker EH, Preis SR, Beiser AS, Wolf PA, Au R, Kloog I, et al. 2015. Long-term exposure to fine particulate matter, residential proximity to major roads and measures of brain structure. Stroke 46(5):1161–1166, PMID: 25908455, https://doi.org/10.1161/STROKEAHA.114.008348.
Wurth R, Kioumourtzoglou MA, Tucker KL, Griffith J, Manjourides J, Suh H. 2018. Fine particle sources and cognitive function in an older Puerto Rican cohort in greater Boston. Environ Epidemiol 2(3):e022, PMID: 30506018, https://doi.org/10.1097/EE9.0000000000000022.
Xu X, Ha SU, Basnet R. 2016. A review of epidemiological research on adverse neurological effects of exposure to ambient air pollution. Front Public Health 4:157, PMID: 27547751, https://doi.org/10.3389/fpubh.2016.00157.
Younan D, Petkus AJ, Widaman KF, Wang X, Casanova R, Espeland MA, et al. 2020. Particulate matter and episodic memory decline mediated by early neuroanatomic biomarkers of Alzheimer's disease. Brain 143(1):289–302, PMID: 31746986, https://doi.org/10.1093/brain/awz348.
Zanchi D, Giannakopoulos P, Borgwardt S, Rodriguez C, Haller S. 2017. Hippocampal and amygdala gray matter loss in elderly controls with subtle cognitive decline. Front Aging Neurosci 9:50, PMID: 28326035, https://doi.org/10.3389/fnagi.2017.00050.